The Influence of Ni and V Trace Elements on High-Temperature Tensile Properties and Aging of A356 Aluminum Foundry Alloy

MARIA TERESA DI GIOVANNI, EMANUELA CERRI, DANIELE CASARI, MATTIA MERLIN, LARS ARNBERG, and GIAN LUCA GARAGNANI

High-temperature tensile properties of unmodified A356 alloy with and without the addition of Ni or V in traces (600 and 1000 ppm of Ni and V, respectively) were investigated by analyzing samples obtained from sand and permanent mold castings in the as-cast and T6 heat-treated conditions. Tensile tests were performed at 508 K (235 °C) at a crosshead speed of 1 mm/min. In addition, samples were subjected to artificial aging at 508 K (235 °C) for different times, and corresponding hardness curves were plotted. Microstructures and fracture surfaces, analyzed by FEG-SEM equipped with energy dispersive X-ray spectroscopy, showed that neither Ni nor V addition had a detrimental effect on high-temperature tensile properties. Aging curves showed a strong loss of hardness affecting the T6 class between 30-min and 1-h exposure time. After 6-h aging, no evidence of aging treatment persisted on hardness of the tested material. Hardness values did not reveal any significant difference between the reference alloy and the Ni- and V-containing alloys in both casting conditions, in complete analogy with the tensile properties. Unmodified eutectic silicon particles provided inhomogeneity in the α-Al matrix and acted as the principal source of stress concentration leading to fracture.

DOI: 10.1007/s11661-016-3366-1

I. INTRODUCTION

IN the last decades, aluminum alloys have been re-focused in terms of lightweight material for vehicles. Replacing cast iron with aluminum alloys can result in a significant weight reduction and consequently better fuel efficiency.[1,2] High-temperature performance is a critical characteristic affecting an alloy's suitability for various automotive power-train applications. Contemporary automotive engines operate at the highest temperatures reaching up to 523 K (250 °C).[3] This creates demanding operating requirements for the existing Al-Si-Cu and Al-Si-Mg alloys that typically lose strength above 423 K (150 °C).[4–7]

Industries have also shown a growing interest in the effect of increased Ni and V levels on the mechanical properties of aluminum alloy products. In fact, the deterioration in the coke quality and, as a result, in the quality of the anodes used in the Hall–Héroult process has led to an increase in the amount of these metal impurities in the downstream products. In the next years, the levels of Ni and V are expected to rise to 420 and 1080 ppm,[8] respectively. At present, there is no cost efficient method available for the removal of these impurities, and the response to the problem is mainly monitoring the Ni and V levels and checking for any negative influence.[9] Therefore, considering the new trends, it might be interesting to understand which role is played by Ni and V additions on the high-temperature mechanical behavior. A previous study investigated the room temperature tensile properties of sand cast and permanent mold cast unmodified A356 alloy containing 600 and 1000 ppm of Ni and V, respectively.[10] It was found that Ni and V strongly affect both the yield strength ($Rp_{0.2}$) and ultimate tensile strength (UTS) of the sand cast alloy in the as-cast condition. In particular, Ni reduces $Rp_{0.2}$ and UTS by 87 and 37 pct, respectively, whereas V increases $Rp_{0.2}$ and UTS by 42 and 25 pct. Hence, the objective of this work is to evaluate the influence of Ni and V trace elements on the high-temperature tensile properties of the unmodified A356 foundry alloy in the as-cast and T6 heat-treated condition, solidified by means of both sand and permanent mold casting processes. High-temperature tensile tests and hardness measurements were performed to assess the mechanical properties.

Observing the small elongation values, it is reasonable to assume that the kinetic of the strain hardening mechanism is mostly ruled by the effect of the temperature than to the effect of dynamic strain. Hence, aging curves were plotted in order to verify if the samples are susceptible to aging at the testing temperature.

MARIA TERESA DI GIOVANNI, Assistant Researcher, and EMANUELA CERRI, Professor, are with Dip. Ingegneria Industriale, Universitá di Parma, v.le G. Usberti 18/A, 43124-Parma, Italy. Contact e-mail: mariateresa.digiovanni@unipr.it. DANIELE CASARI, Postdoctoral Fellow, is with the Dept. of Physics, NTNU, Høgskoleringen 5, N-7491 Trondheim, Norway. MATTIA MERLIN and GIAN LUCA GARAGNANI, Professors, are with the Dip. Ingegneria, Universitá di Ferrara, v. Saragat 1, 44122-Ferrara, Italy. LARS ARNBERG, Professor, is with the Dept. of Materials Science and Engineering, NTNU, A. Getz vei 2, N-7491 Trondheim, Norway.
Manuscript submitted July 21, 2015.

Published online: 17 February 2016

Moreover, microstructure and fracture surfaces were observed by means of Optical Microscopy (OM) and Scanning Electron Microscopy (SEM).

II. EXPERIMENTAL DETAILS

A. *Material*

In this study, the hypoeutectic A356 foundry alloy was used as base alloy. As described in a previous work,[10] the as-received ingots were melted in charges of 16 kg each in a boron nitride-coated clay graphite crucible. Trace elements were added in concentrations of 600 and 1000 ppm of Ni and V, respectively. Neither Sr nor Na was added as modifier agent. Samples from the three different casting trials were obtained and subsequently analyzed by Optical Emission Spectroscopy (OES). The chemical compositions of the A356 reference alloy and the Ni- or V-containing alloys are given in Table I.

B. *Casting and Heat Treatment*

After the melt preparation, the alloys were poured in both sand and steel molds. Sand castings were obtained using an improved version of the tensile testing bars proposed by Dispinar and Campbell.[10,11] The cooling rate in the middle of the sand cast specimen was 1.3 K/s. In accordance with the UNI 3039 specification, an L-shaped steel mold was chosen for the permanent mold castings. The temperature of the die was kept at 573 K (300 °C) during the casting trials. The cooling rate in the middle of the permanent mold cast specimen was 4.2 K/s. Part of the samples originating from both the casting methods were subjected to a T6 heat treatment. They were solubilized at 813 K (540 °C) for 4 hours, quenched in a water bath at 293 K (20 °C), and finally aged at 433 K (160 °C) for 6 hours. Twelve different experimental conditions were investigated (Table II), and at least five specimens were tested for each condition.

C. *High-Temperature Tensile Tests*

High-temperature tensile tests were performed on a MTS 880 universal testing machine (10 tons) equipped with a furnace chamber and a MTS Teststar control unit. All the specimens were tested at 508 K ± 5 K (235 °C ± 5 °C), at a crosshead speed of 1 mm/min and with the applied load restricted to 40 kN. To ensure the thermal stability in the whole specimen, the sample was exposed to the preset temperature for 15 min before the beginning of the test. One dummy specimen was used to directly check the temperature by placing a thermocouple at its center plane. A specifically designed clip-on stainless steel axial extensometer connected to an optical position measuring system was used to collect the stress–strain data.

D. *Microstructure Analysis*

After tensile tests, the specimens were prepared for the microstructural analysis. Samples for fractographic investigation were sectioned parallel to the fracture surface and cleaned in an ultrasonic bath to remove all debris, grease or oils due to the cutting process. Samples for metallographic investigation were sectioned perpendicular to the fracture surface and embedded in a low-viscosity epoxy resin. The grinding procedure was performed by SiC papers, from 320 up to 2400, by applying a force of 15 N for 60 seconds. The samples were then polished using MD-Mol (3 μm) at 15 N for 6 min and subsequently MD-Nap (1 μm) at 15 N for 6 min. Microstructures and fracture surfaces were observed by means of a HITACHI SU-6600 Field Emission Scanning

Table I. Chemical Composition (Weight Percentage) of A356 Reference Alloy and Ni/V-Containing Alloys as Measured by OES

Alloy	Addition (ppm)	Si	Fe	Mg	Ni	V	Al
A356	—	7.054	0.092	0.355	0.003	0.007	bal.
A356 + Ni	600	6.902	0.087	0.344	0.061	0.007	bal.
A356 + V	1000	6.992	0.094	0.349	0.003	0.108	bal.

Table II. Condition Specification of Specimens

Alloy	Mold	Condition	Alloy Code
A356	Sand	as-cast	A356 AC
		T6	A356 T6
A356 + 600 ppm Ni	Sand	as-cast	N AC
		T6	N T6
A356 + 1000 ppm V	Sand	as-cast	V AC
		T6	V T6
A356	Permanent mold	as-cast	A356 PM AC
		T6	A356 PM T6
A356 + 600 ppm Ni	Permanent mold	as-cast	N PM AC
		T6	N PM T6
A356 + 1000 ppm V	Permanent mold	as-cast	V PM AC
		T6	V PM T6

Electron Microscope (FEG-SEM) equipped with Energy Dispersive X-ray Spectroscopy (EDS).

E. *Aging and Vickers Hardness Test*

A set of samples not subjected to mechanical test underwent Vickers Hardness Test. Cylindrical samples about 1 cm in diameter were cut and artificially aged at 508 K ± 3 K (235 °C ± 3 °C) to determine the aging curves. The exposure times were 5, 10, 15, 20, 30 minutes, 1, 2, 4, and 6 hours. After aging, hardness samples were ground flat and testing surfaces where finished with 1200 SiC paper. Vickers microhardness tests (HV) were performed in the center of the cylindrical samples' base at a load of 300 g and a dwell time of 15 s, according to UNI EN ISO 6507 specification.

III. RESULTS AND DISCUSSION

A. *High-Temperature Tensile Properties*

Figures 1 and 2 collect the average values of the high-temperature tensile properties of the sand cast and permanent mold cast alloys. No relevant differences between the reference alloy and the Ni- and V-containing alloys were found in both casting conditions. This indicates that neither Ni nor V addition influences the high-temperature mechanical behavior. Yield strength ($Rp_{0.2}$) and ultimate tensile stress (UTS) data have small error bars, indicating the reproducibility and the reliability of the data, whereas elongation (A pct) error bars are slightly larger.

Figure 1 summarizes the high-temperature tensile properties of the sand cast alloys (A356 and Ni/V-containing alloys), in the as-cast (Figure 1(a)) and in the T6 condition (Figure 1(b)) respectively. With respect to the sand cast case, the precipitation of fine coherent Mg_2Si particles in the α-Al matrix, promoted by the T6 heat treatment, exerts a strong effect on the strength of the material.[12] This is clearly indicated by the remarkable increase in $Rp_{0.2}$ and UTS by 78 and 54 pct, respectively, compared to the as-cast samples.

The coherent Mg_2Si precipitates with their needle-like shape can counteract the glide of dislocations, which accumulate and significantly strengthen the α-Al matrix. Despite this improvement, the α-Al matrix is more easily

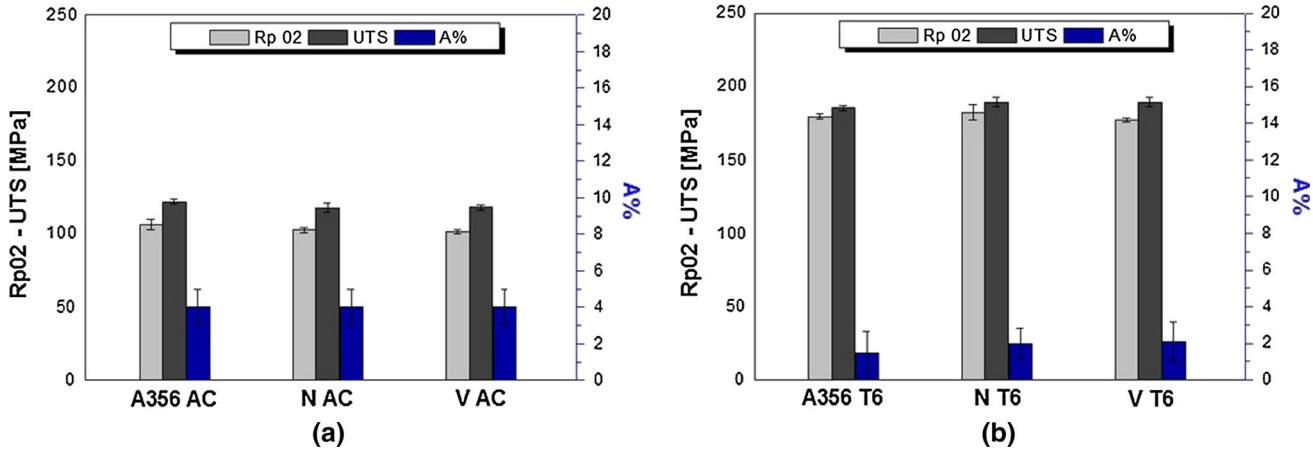

Fig. 1—High-temperature tensile properties of the sand cast A356 reference and Ni/V-containing alloys (*a*) in the as-cast condition and (*b*) in the T6 condition.

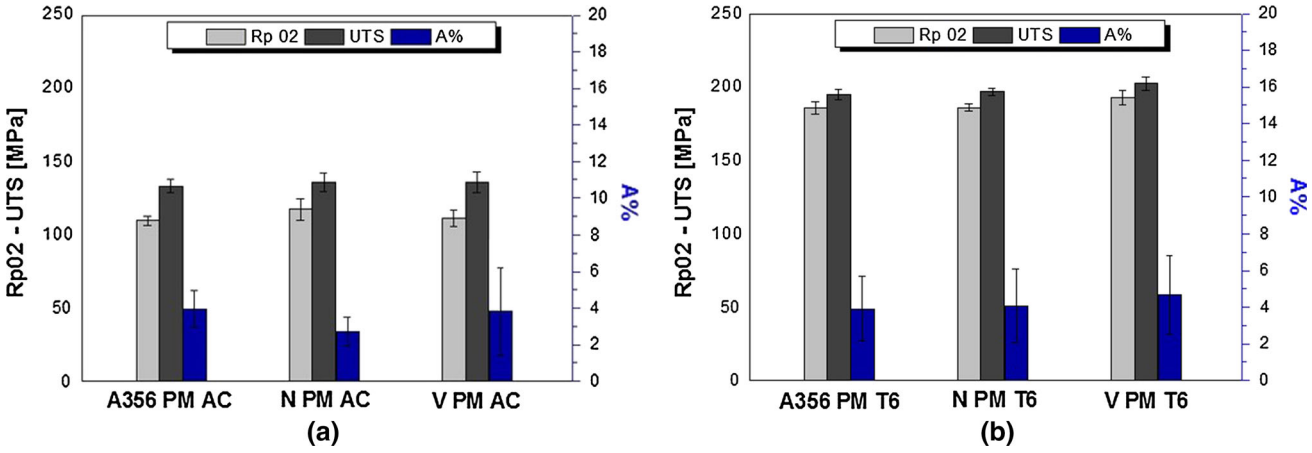

Fig. 2—High-temperature tensile properties of the permanent mold reference and Ni/V-containing alloys (*a*) in the as-cast condition and (*b*) in the T6 condition.

susceptible to cracking. As a result, when the fracture of the brittle eutectic particles begins, the propagation of crack through the matrix is easier, requiring a lower amount of energy. This leads to a remarkable reduction in the ductility (in terms of elongation A pct) of the T6 treated alloy compared to the corresponding as-cast alloy.

Moreover, the as-cast specimens show a lower $Rp_{0.2}$/UTS ratio than the T6 treated samples. This is probably due to the presence of reinforcing precipitates that block the motion of the dislocations and lead the heat-treated material to require higher stress to yield.

Figure 2 summarizes tensile test results at 508 K (235 °C) for the permanent mold cast alloys, in both the as-cast (Figure 2(a)) and T6 conditions (Figure 2(b)). Comparing the T6 heat-treated samples with the as-cast ones, $Rp_{0.2}$ and UTS increase by 65 and 47 pct, respectively. Considering the analogy with the sand cast case, the effect of precipitation hardening on the tensile properties and Rp $_{0.2}$/UTS ratio at elevated temperature will not be discussed.

With respect to A pct, it is observed that the ductility improvement linked to the necking and spheroidization of eutectic Si particles during the solubilization stage (Figures 2(a) and (b)) is negligible.

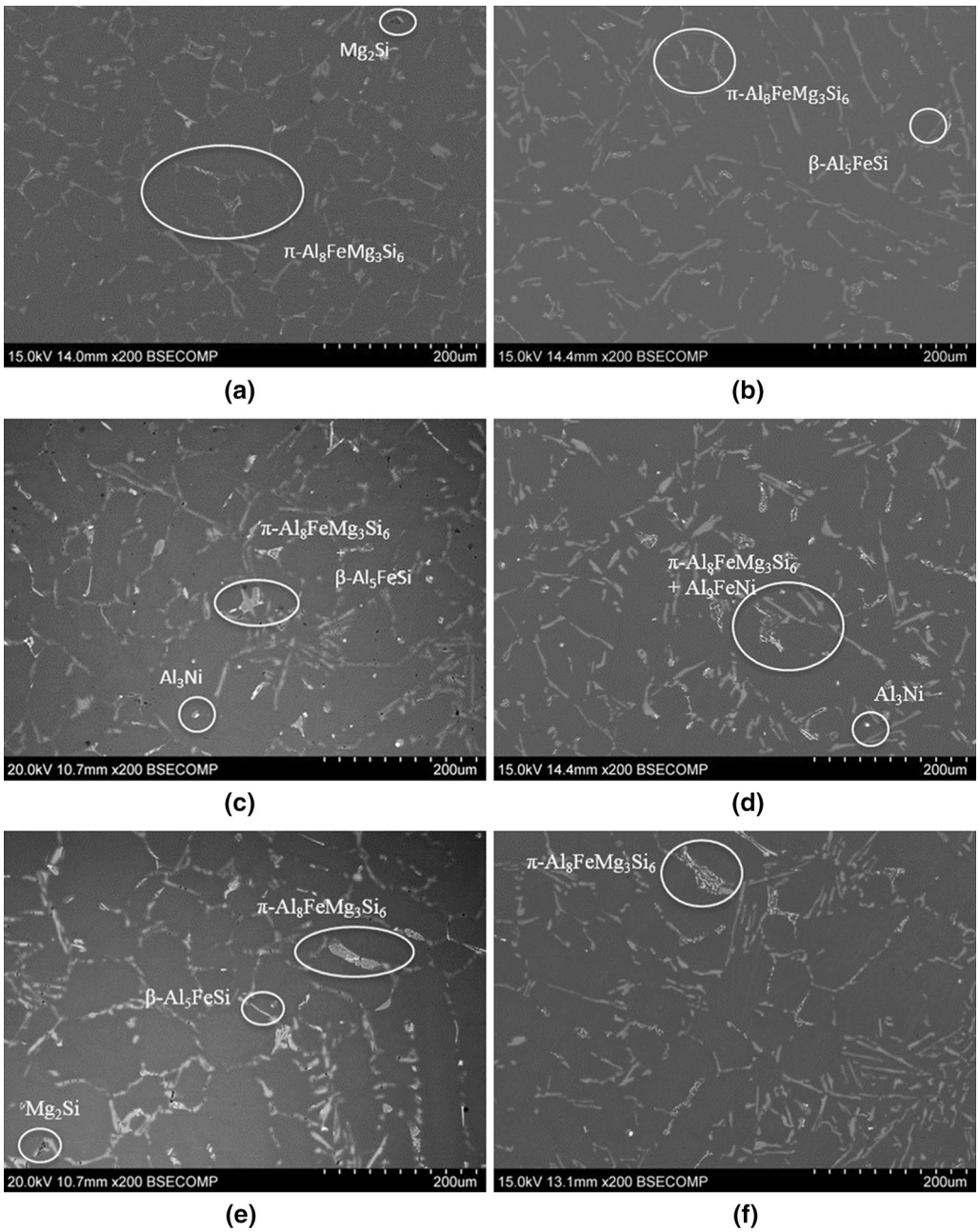

Fig. 3—BSE micrographs of sand cast reference, Ni- and V-containing alloys in as-cast and T6 conditions tested at elevated temperature: (*a*) A356 AC, (*b*) A356 T6, (*c*) N AC, (*d*) N T6, (*e*) V AC, (*f*) V T6. Aluminum dendrites are in dark gray, eutectic Si crystal in light clear gray, π-Al8FeMg3Si6 and β-Al5FeSi in light clear gray, Mg2Si in black, and Ni-rich intermetallics in white.

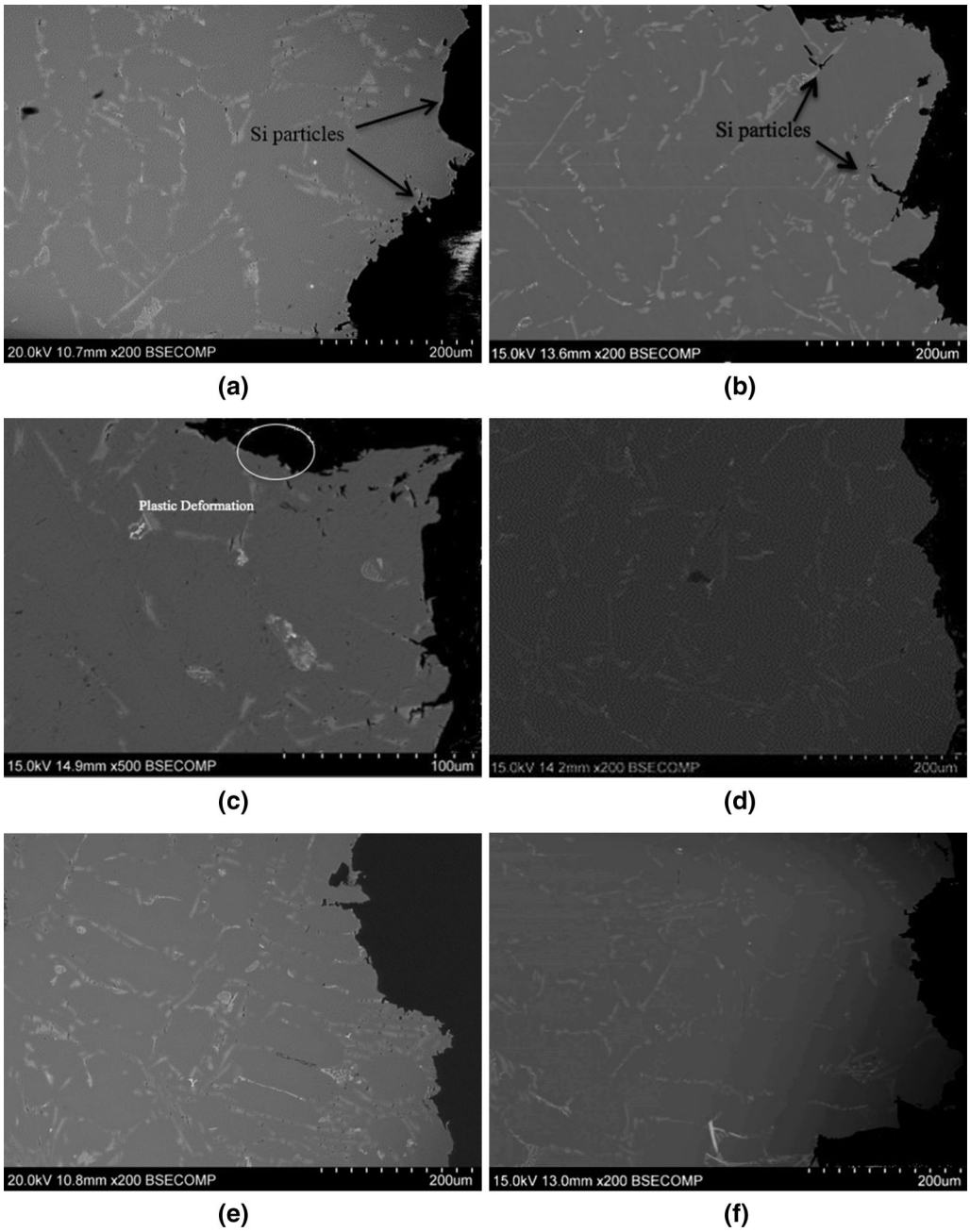

Fig. 4—BSE micrographs of the fracture profile of sand cast A356 reference, Ni-, and V-containing alloys in the as-cast and T6 conditions tested after high-temperature tensile test: (*a*) A356 AC, (*b*) A356 T6, (*c*) N AC, (*d*) N T6, (*e*) V AC, (*f*) V T6. A Si-driven quasi-cleavage and matrix crack are the main fracture mode. No significant differences between crack paths of the as-cast and T6 heat-treated alloys are observed.

A lower $Rp_{0.2}$/UTS ratio is observed in the permanent mold samples compared to the sand cast samples mostly due to the higher ultimate tensile strength resulting from this casting technology. In general, mechanical properties of the permanent mold tensile samples are higher than those obtained for the sand cast alloys, although the increase is not substantial (average increments range from 3 to 15 MPa for $Rp_{0.2}$ and from 7 to 18 MPa for UTS). It is worth noting, however, that $Rp_{0.2}$ data do not overlap one another except for a couple of conditions, *i.e.*, for the A356 AC and N T6 alloys, while UTS data never overlap. Hence, the slight increases in $Rp_{0.2}$ and UTS are statistically relevant and can reasonably be ascribed to the microstructure obtained through permanent mold casting, which offers a less segregated eutectic structure having smaller and more homogeneously distributed Si particles. Nonetheless, it is evident that the solidification microstructure has less influence than Mg_2Si precipitation hardening on $Rp_{0.2}$ and UTS.

Concerning the A pct, comparisons between Figures 1(b) and 2(b) and between Figures 2(a) and (b) show that the higher cooling rate of permanent mold casting effectively counteracts the ductility reduction linked to Mg_2Si precipitation. In the absence of casting defects,

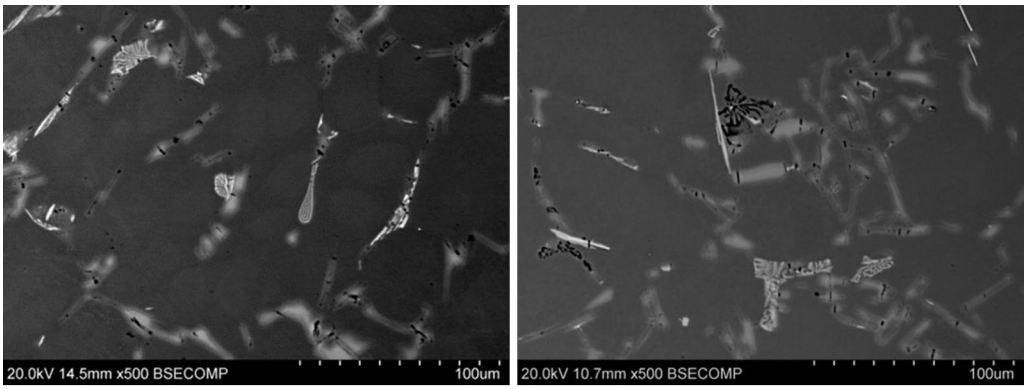

Fig. 5—BSE micrographs of the non-treated sand cast A356 alloy close to the fracture surface, showing Si particles and Fe-bearing compounds cracked.

ductility of A356 alloys is controlled by SDAS and size and aspect ratio of eutectic Si particles, which are strongly dependent on the cooling rate.[13] The increase of the cooling rate during solidification decreases the SDAS and subsequently divides the eutectic liquid into many small pockets rather than the large eutectic regions present in the low cooling rate structure.[10] A finer structure with smaller and more rounded particles, as well as long dislocation slipping distances within the grains, results in a lower particle cracking rate and hence a higher ductility.[14]

B. *Microstructural Analysis*

Microstructural investigations were performed by analyzing the fracture profiles of the samples. Backscattered electron (BSE) images of the A356 reference alloys as well as of Ni- and V-containing alloys in the as-cast and T6 heat-treated conditions are shown in Figure 3. For the sake of clarity, only the sand cast samples are presented. The main features are α-Al dendrites and needle-like Si eutectic particles. Fe-bearing phases such as π-$Al_8FeMg_3Si_6$ and β-Al_5FeSi, Ni-rich intermetallic compounds (Al_3Ni and Al_9FeNi), as well as Mg_2Si particles are also observed. In the eutectic region, platelet-like β-Al_5FeSi intermetallics are occasionally found associated with the "Chinese Script" π-$Al_8FeMg_3Si_6$ phase (Figure 3(c)). Ni-based intermetallics phases, exhibiting a polyhedral shape, are observed in the sand cast alloy with Ni addition (Figures 3(c) and (d)). A slight increase in the amount of π-$Al_8FeMg_3Si_6$ and Mg_2Si intermetallic compounds is observed in the V-containing samples (Figures 3(e) and (f)). As reported,[10] this may be related to a competition with Mg as a solid solution element in α-Al matrix. By entering solid solution, V allows more Mg to be available in the remaining liquid during solidification, which in turn yields to a larger amount of Mg-containing intermetallics in the eutectic region. A moderate spheroidization of eutectic Si particles is noted in the T6 heat-treated samples due to solution heat treatment. Fe-bearing compounds have a more marked tendency to spheroidize, as shown in Figures 3(b) and (d).

C. *Fractographic Observations*

Figure 4 shows the fracture profile of the A356 reference alloy (Figures 4(a) and (b)), Ni-containing (Figures 4(c) and (d)) and V-containing (Figures 4(e) and (f)) alloys in the as-cast and T6 heat-treated conditions. It is evident that the fracture path mainly follows the eutectic region, as indicated by the arrows in Figures 4(a) and (b). A significant plastic deformation of α-Al dendrites is also noticed in all the investigated alloys (Figure 4(c)). Below the main fracture, multiples cracks oriented perpendicularly to the applied stress are observed in both Si particles and Fe-bearing phases (Figure 5). Similar fracture paths are observed in the T6 heat-treated alloys.

SEM micrographs of the fracture surfaces (Figure 6) are in line with room-temperature findings[10] and confirm the Si-driven quasi-cleavage nature of the fracture, as evidenced by the number of cleavage planes and brittle Si flakes. Few dimples are detected, as shown in Figures 6(a) and (b).

In the absence of modifier elements such as Sr or Na, the selected solution heat treatment holding time appears to be insufficient to obtain complete necking and spheroidization of the Si particles. In fact, the majority of eutectic Si crystals still show an elongated acicular morphology. These elongated particles, acting as the principal source of stress concentration, generally initiate fracture.[15,16] Larger eutectic silicon particles cluster along both cell and grain boundaries generating a nearly continuous wall of eutectic silicon particles around the dendrite cell. Microcracks originated in those Si particles propagate through the α-Al matrix and subsequently connect to each other to produce the main crack.

The examined alloys behave as a composite material where the harder intermetallics and eutectic Si particles (high Young's Modulus E) generally reinforce the soft matrix (low E) by bearing the main part of the applied

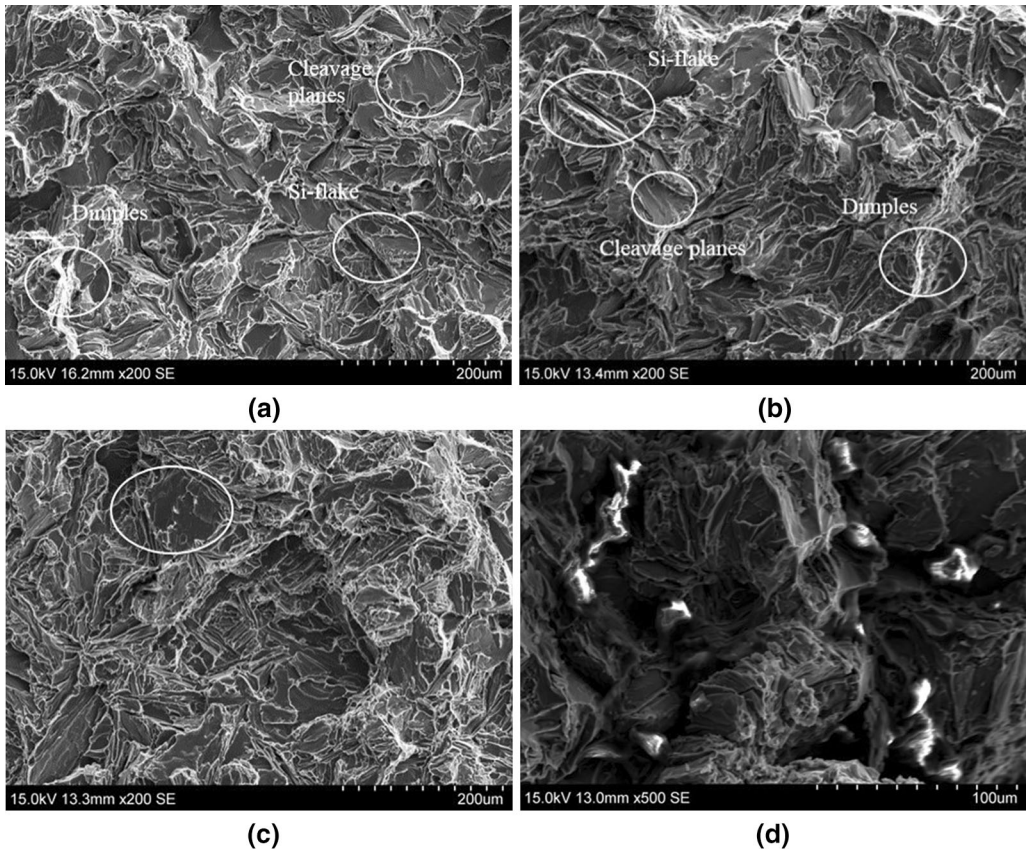

Fig. 6—BSE micrographs of the fracture surfaces of sand cast A356 reference in the as-cast (*a*) and T6 conditions (*b*) tested after high-temperature tensile test showing the typical features of ductile–brittle mixed fracture. The flake-like morphology of Si particles persists after the solution heat treatment. Ni-rich intermetallics compounds detected in a sand cast as-cast alloy with 600 ppm Ni (*c*), (*d*).

load. When these materials are subject to external loads, the difference in the nature of the component produces an inhomogeneity in the stress distribution. If the stress induced at the particles or at the matrix–particles interface exceeds a critical value, then fracture of the particles or decohesion occurs.[17,18] At high temperatures, the α-Al matrix is more prone to deformation, which implies that internal stresses originated by the structural inhomogeneity can be partially recovered at the expense of the matrix. As a result, fracture occurs at lower UTS values compared with the room-temperature case,[10] but at generally higher A pct.

After T6 heat treatment, the precipitation of fine coherent Mg_2Si phases in the α-Al matrix exerts a strong effect on the tensile properties of both the sand cast and permanent mold cast samples. Despite this improvement, the α-Al matrix is prone to crack more easily due to the hardening particles. In fact, when the fracture of brittle particles begins, the following microcrack linking process is faster and leads to a slightly lower ductility compared to the corresponding as-cast alloys.[10] In order to offer a comprehensive evaluation of the influence of Ni and V trace elements on the mechanical properties, their effect on the microstructure (when evident) is reported. Ni-rich intermetallics compounds are detected in sand cast alloys with 600 ppm Ni (Figures 6(c) and (d)).

D. *Aging and Vickers Hardness Evaluation*

Vickers hardness tests were carried out in order to endorse the hypothesis of artificial aging occurred during the high-temperature tensile tests. The poor ductility exhibited by the alloys in all the experimental conditions (Figures 1 and 2) allowed us to compare the aging occurring in static condition to the one achieved through the tensile test at elevated temperature, where it is reasonable to assume that the kinetic of the strain hardening mechanisms is mostly ruled by the effect of the temperature than by dynamic strain. Vickers Hardness measurements were obtained after aging the A356 base alloy and the Ni- and V-containing alloys at 508 K (235 °C) (testing temperature) with different aging times (Figure 7). The first values (t = 1 s) are representative of the as-given samples, which are taken as reference values for the aging evaluation.

Vickers Hardness curves are organized as follows: on the left side the as-cast samples, sand (Figure 7(a)) and permanent mold (Figure 7(c)) casting methods; on the right side the T6 heat-treated samples, sand (Figure 7(b)) and permanent mold (Figure 7(d)) casting techniques.

At t = 1 s, the as-cast and T6 samples poured in the permanent mold present slightly higher hardness values (~5, ~3HV) than the sand cast samples, in agreement

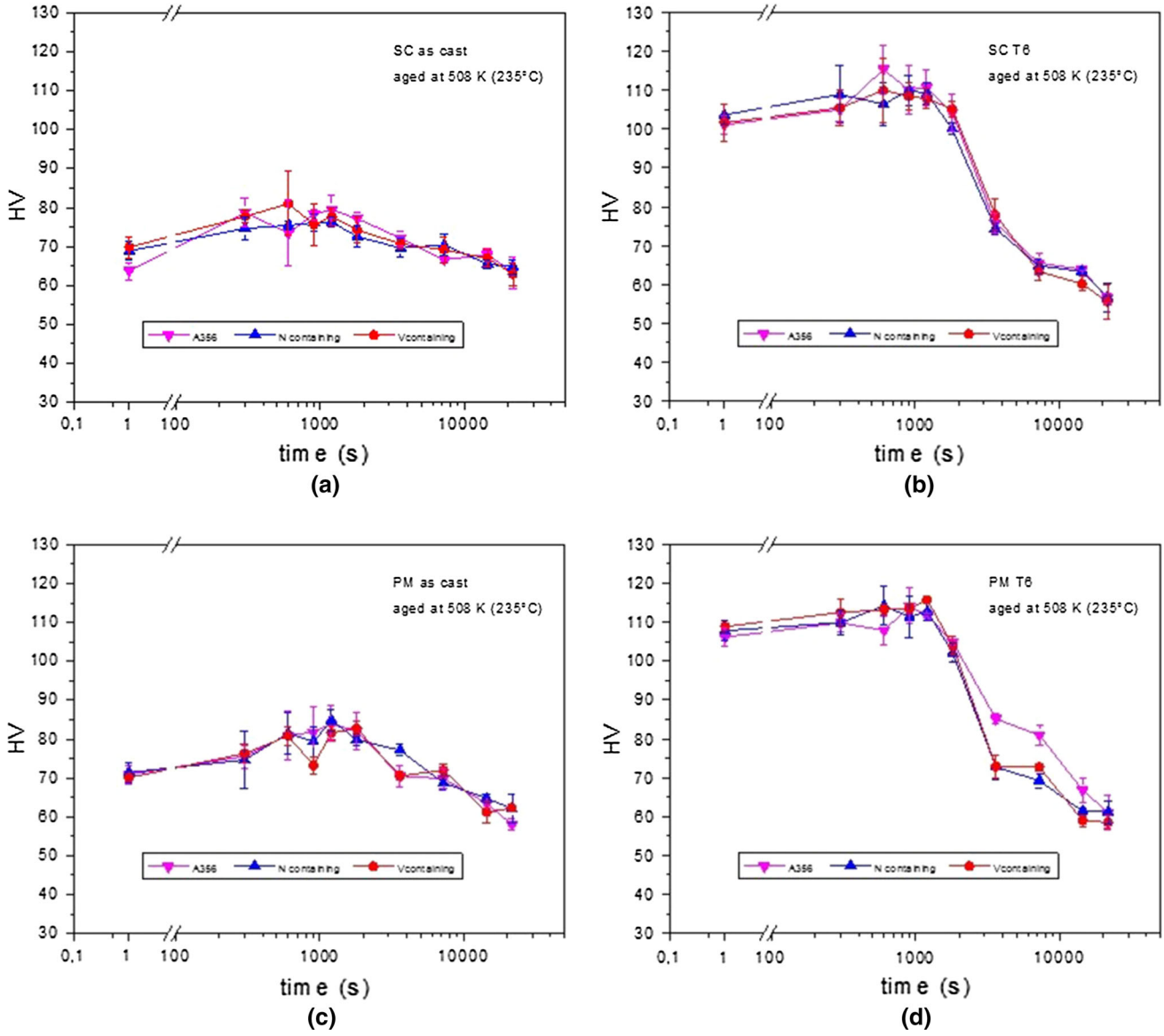

Fig. 7—Aging curves at 508 K (235 °C) for the A356 reference, Ni- and V-containing alloys in the 4 different experimental conditions: (*a*) sand cast as-cast, (*b*) sand cast T6, (*c*) permanent mold as-cast, (*d*) permanent mold T6.

with the tensile values presented in.[10] After a 5-min aging time, a clear strengthening is observed for each experimental condition. The effect becomes more evident after 10 and 20 minutes, where the as-cast and the T6 classes achieve their hardness peak, respectively.

The alloys in the T6 condition are subjected to a strong hardness decrease. After a 6-hour aging, an average reduction of 56 and 60 HV (approximately 50 pct lower than the peak hardness) can be observed for the sand cast and permanent mold cast alloys, respectively. In contrast, the alloys in the as-cast condition exhibit a smoother hardness variation: after the peak values of 75 HV (sand cast) and 82 HV (permanent mold), a slight decrease in hardness by 16 and 25 pct is observed at 6 hours aging, and minimum values of 63 HV (sand cast) and 61 HV (permanent mold) are measured.

It is worth noting that the as-cast samples did not receive any solution treatment before aging. Therefore, the strengthening attained during this process, depending on the volume fraction and the size of the particles precipitated and on the nature of the interaction of the particles with dislocations, is based on the presence of metastable Mg and Si atoms in the solidified α-Al matrix. Hence, the increase in yield strength at high temperature, as compared to room-temperature experiments,[10] could be attributed to the artificial aging activated during tensile test [15 min + test duration at 508 K (235 °C)].

As far as the T6 heat-treated alloys are concerned, a strong loss of hardness is evidenced between 30-minutes and 1-hour exposure time. This might be a serious concern for industrial engine applications, where temperatures commonly exceed 473 K (200 °C).

In accordance with previous findings,[19] it is confirmed that the hardness and thus the mechanical properties of peak-aged[20,21] T6 heat-treated castings could be further modified by the in service conditions of the component, especially after prolonged high-temperature exposure. It is also reasonable to affirm that the combination of temperature [508 K (235 °C)] and duration time (15 min + test duration) of high-temperature tensile tests yields an over-aging of the alloys. In this study, the over-aging was demonstrated through a combination of tensile and hardness tests. However, in order to analyze the microstructural evolution of the Mg_2Si precipitate, a Transmission Electron Microscopy investigation is recommended. With the exception of the A356 PM T6 alloy (Figure 7(d)), the comparison of hardness values did not reveal any significant difference between the reference alloy and the Ni/V-containing alloys in both casting conditions, in complete agreement with the tensile properties.

IV. CONCLUSIONS

The influence of Ni and V trace elements on the high-temperature tensile properties of the unmodified A356 aluminum foundry alloy in the as-cast and T6 heat-treated conditions was assessed. Both sand and permanent mold casting processes were taken into account. High-temperature tensile tests and Vickers hardness measurements were performed to evaluate the mechanical properties. Further, microstructural and fractographic investigations were carried out to analyze the microstructural features involved in the fracture process. The following conclusions can be drawn from this study:

1. No differences in high-temperature tensile properties are observed between the A356 reference alloy and the Ni- and V-containing alloys.
2. Owing to the finer microstructure, a slight increase in yield strength ($Rp_{0.2}$), ultimate tensile strength (UTS), and elongation (A pct) is found in the permanent mold cast alloys compared to the sand cast alloys.
3. The T6 heat treatment is more efficient than the permanent mold casting technique in terms of mechanical reinforcement.
4. The combination of temperature [508 K (235 °C)] and duration time (15 min + test duration) of high-temperature tensile tests can lead to an over-aging of the alloys.
5. Aging curves show a significant loss of hardness in the T6 alloys between 30-min and 1-hour exposure time at [508 K (235 °C)]. After 6 hours of aging, no evidence of heat treatment is observed in the investigated alloys. This might be a serious issue for industrial engine applications, where temperatures commonly exceed 473 K (200 °C).
6. SEM investigations of the fracture profiles and surfaces highlight the Si-driven quasi-cleavage nature of the fracture, as proved by the number of cleavage planes and brittle Si flakes. Few dimples are detected in the fracture surfaces. No significant differences in the fracture paths are observed between the as-cast and the T6 heat-treated alloys.

ACKNOWLEDGMENTS

The authors thank Thomas Hartmut Ludwig for helpful discussions. In addition, the authors gratefully acknowledge Hydro Aluminium AS (Norway) for the financial support. The authors also thank Hermann Hovland from Sør-Norge Aluminium AS (Norway) for the supply of master alloys, and Arne Nordmark and Kurt Sandaunet for their help during the production of castings.

REFERENCES

1. W. Kasprzak, D. Emadi, M. Sahoo, and M. Aniolek: *Mater. Sci. Forum*, 2009, vols. 618–619, pp. 595–600.
2. R. Dhingra and S. Das: *J Clean Prod.*, 2014, vol. 85, pp. 347–58.
3. W. Kasprzak, Z. Deng, J. Powell, M. Niewczas: *JILM*, 2010, pp. 669–74.
4. R. Molina, P. Amalberto, and M. Rosso: *Metall. Sci. Tech.*, 2011, vols. 29–1, pp. 5–15.
5. R. Molina, P. Amalberto, and M. Rosso: *Metall. Sci. Tech.*, 2011, vols. 29–2, pp. 5–13.
6. Z. Asghar, G. Requena, and F. Kubel: *Mater. Sci. Eng. A*, 2010, vol. 527, pp. 5691–98.
7. Y. Li, Y. Yang, Y. Wu, L. Wang, and X. Liu: *Mater. Sci. Eng. A*, 2010, vol. 527, pp. 7132–37.
8. G. Jha, S. Ningileri, X. Li, R. Bowers, B. Sadler (eds.), *Light Metals*, Wiley, New Jersey, 2013, pp. 929–34.
9. J. Grandfield and J. Taylor: *Mater. Sci. Forum*, 2009, vol. 630, pp. 129–36.
10. D. Casari, T.H. Ludwig, L. Arnberg, M. Merlin, and G.L. Garagnani: *Mater. Sci. Eng. A*, 2014, vol. 610, pp. 414–26.
11. D. Dispinar and J. Campbell: *Mater. Sci. Eng. A*, 2011, vol. 528, pp. 3860–65.
12. G.E. Dieter: *Mechanical Metallurgy*, 3rd ed., Mc Graw-Hill Book Co., New York, 1986, pp. 188–228.
13. Q.G. Wang: *Metall. Mater. Trans. A*, 2003, vol. 34A, pp. 2887–99.
14. S.G. Shabestari and F. Shahri: *J. Mater. Sci.*, 2004, vol. 39, pp. 2023–32.
15. Q.G. Wang, C.H. Casaeres, and J.R. Grifhits: *Metall. Trans. A*, 2003, vol. 34A, pp. 2901–12.
16. I. Fadavi, A. Boostani, and S. Tamanthas: *J. Alloys Compd.*, 2009, vol. 481 (1–2), pp. 220–27.
17. I. Sinclair and P.J. Gregson: *Mater. Sci. Techonol.*, 1997, vol. 13, pp. 709–26.
18. M. Huang and Z. Li: *Int. J. Solid. Struct.*, 2009, vol. 43, pp. 634–41.
19. B. Baradarani and R. Raiszadeh: *Mater. Des.*, 2011, vol. 32, pp. 935–40.
20. P.A. Rometsch and G.B. Schaffer: *Mater. Sci. Eng. A*, 2002, vol. 325, pp. 424–34.
21. *Metals Handbook*, 2 Edn, *Heat Treating of Nonferrous Alloys*, 1998, p. 1035.